

Negative correlations between cultivable and active-yet-uncultivable pyrene degraders explain the postponed bioaugmentation

Bo Jiang, Yating Chen, Yi Xing, Luning Lian, Yaoxin Shen, Baogang Zhang, Han Zhang, Guangdong Sun, Junyi Li, Xinzi Wang, Dayi Zhang



PII: S0304-3894(21)02157-9

DOI: <https://doi.org/10.1016/j.jhazmat.2021.127189>

Reference: HAZMAT127189

To appear in: *Journal of Hazardous Materials*

Received date: 18 June 2021

Revised date: 6 September 2021

Accepted date: 7 September 2021

Please cite this article as: Bo Jiang, Yating Chen, Yi Xing, Luning Lian, Yaoxin Shen, Baogang Zhang, Han Zhang, Guangdong Sun, Junyi Li, Xinzi Wang and Dayi Zhang, Negative correlations between cultivable and active-yet-uncultivable pyrene degraders explain the postponed bioaugmentation, *Journal of Hazardous Materials*, (2021) doi:<https://doi.org/10.1016/j.jhazmat.2021.127189>

This is a PDF file of an article that has undergone enhancements after acceptance, such as the addition of a cover page and metadata, and formatting for readability, but it is not yet the definitive version of record. This version will undergo additional copyediting, typesetting and review before it is published in its final form, but we are providing this version to give early visibility of the article. Please note that, during the production process, errors may be discovered which could affect the content, and all legal disclaimers that apply to the journal pertain.

# **Negative correlations between cultivable and active-yet-uncultivable pyrene degraders explain the postponed bioaugmentation**

Bo Jiang<sup>1,2,3</sup>, Yating Chen<sup>1,2</sup>, Yi Xing<sup>1,2</sup>, Luning Lian<sup>1,2</sup>, Yaoxin Shen<sup>1,2</sup>, Baogang Zhang<sup>4</sup>, Han Zhang<sup>4</sup>, Guangdong Sun<sup>5</sup>, Junyi Li<sup>6</sup>, Xinzi Wang<sup>5</sup>, Dayi Zhang<sup>7,\*</sup>

<sup>1</sup> School of Energy and Environmental Engineering, University of Science & Technology Beijing, Beijing 100083, PR China

<sup>2</sup> Beijing Key Laboratory of Resource-oriented Treatment of Industrial Pollutants, University of Science & Technology Beijing, Beijing 100083, PR China

<sup>3</sup> National Engineering Laboratory for Site Remediation Technologies, Beijing 100015, PR China

<sup>4</sup> School of Water Resources and Environment, MOE Key Lab Groundwater Circulation and Environment Evolution, China University of Geosciences, Beijing 100083, PR China

<sup>5</sup> School of Environment, Tsinghua University, Beijing 100084, PR China

<sup>6</sup> Department of Research and Development, Yiqing (Suzhou) Environmental Technology Co. Ltd, Suzhou 215163, PR China

<sup>7</sup> College of New Energy and Environment, Jilin University, Changchun 130021, PR China

## **\*Corresponding author**

Dr Dayi Zhang, College of New Energy and Environment, Jilin University, Changchun 130021, PR China, email: zhangdayi@tsinghua.org.cn

## Abstract

Bioaugmentation is an effective approach to remediate soils contaminated by polycyclic aromatic hydrocarbon (PAHs), but suffers from unsatisfactory performance in engineering practices, which is hypothetically explained by the complicated interactions between indigenous microbes and introduced degraders. This study isolated a cultivable pyrene degrader (*Sphingomonas* sp. YT1005) and an active pyrene degrading consortium (*Gp16*, *Streptomyces*, *Pseudonocardia*, *Panacagrimonas*, *Methylotenera* and *Nitrospira*) by magnetic-nanoparticle mediated isolation (MMI) from soils. Pyrene biodegradation was postponed in bioaugmentation with *Sphingomonas* sp. YT1005, whilst increased by 30.17% by the active pyrene degrading consortium. Pyrene dioxygenase encoding genes (*nidA*, *nidA3* and PAH-RHD $\alpha$ -GP) were enriched in MMI isolates and positively correlated with pyrene degradation efficiency. Pyrene degradation by *Sphingomonas* sp. YT1005 only followed the phthalate pathway, whereas both phthalate and salicylate pathways were observed in the active pyrene degrading consortium. The results indicated that the uncultivable pyrene degraders were suitable for bioaugmentation, rather than cultivable *Sphingomonas* sp. YT1005. The negative correlations between *Sphingomonas* sp. YT1005 and the active-yet-uncultivable pyrene degraders were the underlying mechanisms of bioaugmentation postpone in engineering practices.

**Keywords:** Bioaugmentation, pyrene, soils, magnetic nanoparticle-mediated isolation (MMI), degradation pathway

## 1. Introduction

Polycyclic aromatic hydrocarbons (PAHs) are a typical group of persistent organic pollutants (POPs) containing two or more combined aromatic rings in linear, angular or cluster arrangements (Ghosal, et al., 2016). As natural constituents in fossil fuels, PAHs are present with high concentrations at sites with petroleum refining and transportation activities (Kanaly and Harayama, 2000). At least 600 of 1,408 most severely contaminated sites in USA are contaminated with PAHs (Duan, et al., 2015). Additionally, PAHs can migrate into soils through dry and wet atmospheric deposition (Nam, et al., 2008, Wang, et al., 2017a), and soils are able to attenuate PAHs transport and serve as major sinks (Liu, et al., 2019, Okere, et al., 2017). Moreover, soil PAHs can enter the food chain through bioaccumulation, imposing serious threats to human health (Kim, et al., 2013, Wang, et al., 2017b). Thus, PAHs have gained great attention in recent decades for their ubiquitous presence in environment and high resistance to degradation.

Bioremediation is known as a cost-efficient and environmentally friendly approach to degrade soil pollutants, with low risks in secondary pollution (Haleyur, et al., 2018, Peng, et al., 2008). PAH-degrading bacteria are capable of metabolizing various PAHs via enzymatic attacks on different carbon positions (Segura, et al., 2017, Zeng, et al., 2017). PAH ring hydroxylating dioxygenase (PAH-RHD) are responsible for the initial step of PAHs metabolism (Cebren, et al., 2008), and the encoding genes include *ahd* (Pinyakong, et al., 2003), *dox* (Denome, et al., 1993), *flnA1/A2* (Schuler, et al., 2008), *nag* (Izmalkova, et al., 2013), *nahR* (Bosch, et al., 2000), *nar* (Liu, et al., 2011), *nidA/B* (Stingley, et al., 2004), *nidA3* (Chen, et al., 2016), *pah* (Takizawa, et al., 1999), *pdo* (Krivobok, et al., 2003), *phd* (Saito, et al., 1999) and *phn* (Izmalkova, et al., 2013).

Pyrene is a typical PAH for its similar structure to several carcinogenic PAHs (Peng, et al., 2008). Pyrene biodegradation has been intensively studied, either as carbon and energy source, or as a non-growth substrate in co-metabolism (Johnsen, et al., 2005, Nzila, 2013). Pyrene degraders include *Acinetobacter* (Jiang, et al., 2018b), *Burkholderia* (Vaidya, et al., 2017), *Bacillus* (Rabodonirina, et al., 2018), *Klebsiella* (Elyamine, et al., 2021), *Kocuria* (Sakshi, et al., 2021), *Mycobacterium* (Elyamine, et al., 2021, Wu, et al., 2019), *Pseudomonas* (Elyamine, et al., 2021, Khan, et al., 2018), *Rhodococcus* (Jia, et al., 2019, Sakshi, et al., 2021) and *Sphingomonas* (Guo, et al., 2017).

Bioaugmentation is a practical strategy to improve bioremediation performance at contaminated sites by introducing competent strains or consortia capable of degrading target contaminants (Perelo, 2010). For instance, bioaugmentation with autochthonous *Acinetobacter tandoii* LJ-5 significantly improved phenanthrene removal efficiency by changing the diversity of phenanthrene degraders (Li, et al., 2018a). Other strains in bioaugmentation for PAH degradation include *Klebsiella pneumonia* (Mohanrasu, et al., 2018) and *Acinetobacter johnsonii* (Jiang, et al., 2018b). Although several field studies have demonstrated the feasibility of bioaugmentation to enhance bioremediation performance in groundwater (Major, et al., 2002), wastewater (Wu, et al., 2018) and aquifer (Dybas, et al., 2002), scaling up from laboratory to commercial-scale field is always a challenge. Both abiotic (temperature, moisture, pH, organic matter, aeration, nutrient and soil type) (Heinaru, et al., 2005) and biotic factors (competition between indigenous and exogenous microorganisms for limited nutrients) (Mrozik and Piotrowska-Seget, 2010, Sørensen, et al., 1999) influence bioaugmentation performance. Additionally, the mechanisms of bioaugmentation are

argued (Thompson, et al., 2005), and little is known about the interactions of the introduced degraders with indigenous microbes during bioaugmentation process.

Although cultivation approaches have isolated many PAH degraders, only around 1% (Kaeberlein, et al., 2002, Vartoukian, et al., 2010) or slightly more proportions (Martiny, 2019) of soil microorganisms are cultivable under artificial conditions. Stable isotope probing (SIP) is a well-developed approach to identify functional-yet-uncultivable microorganisms *in situ* (Jiang, et al., 2018a), which however, relies on the isotope incorporation in the active degraders and in most cases cannot isolate living degraders suitable for bioaugmentation. Although SIP coupled with single cell technologies could help in isolating the functional-yet-uncultivable microorganisms for bioaugmentation, the following cultivation step is still challenging for engineering purposes (Wang, et al., 2016b). Recently, a novel technique, magnetic-nanoparticles (MNPs) mediated isolation (MMI), is innovated and aims at separating active degraders from inert bacteria by magnetic gradient (Zhang, et al., 2015, Zhao, et al., 2016). This isotope-independent approach MMI can isolate the active degraders from complex environment in a cost-effective manner. Importantly, the separated microbes remain viable to be used in bioaugmentation (Sun, et al., 2021).

In the present study, both pure cultivation and MMI approaches were applied to isolate pyrene degraders from an abandoned steel plant site. Using cultivable pyrene degrader *Sphingomonas* sp. YT1005 and MMI-enriched active pyrene-degrading consortium in bioaugmentation, we analyzed the pyrene degradation efficiency, metabolic pathway, and pyrene dioxygenase encoding genes. With the hypothesis that microbial intra-correlations play critical roles in pyrene degradation process and affect pyrene metabolism, this work aims to investigate the bioaugmentation performance with

cultivable pyrene degraders, unravel the active pyrene degraders via MMI, explore the bacterial interactions during bioaugmentation process, and explain the underlying mechanisms leading to the postponed bioaugmentation. As the first study to separate and introduce the active pyrene-degrading microbes in soil bioaugmentation, this work can broaden our knowledge on the influential factors affecting bioaugmentation performance and provide novel ideas for improving bioaugmentation performance.

## **2. Materials and methods**

### *2.1. Soil sample*

Soil samples were collected at an abandoned site of Capital Steel Plant located in Shijingshan District, Beijing. This site was severely contaminated by PAHs and the PAHs concentration ranged from several to over 500 mg/kg. One kilogram of soils was obtained from the surface layer (0-20 cm) in the absence of PAHs contamination, stored at 4°C and transferred to laboratory. After homogenization, stones and plant debris were removed. Soil geochemical properties were analyzed and listed in Table S1 (Supporting Information). There was no detectable PAHs in the collected soils and the limits of detection and quantification of PAHs are listed in Table S2 (Supporting Information).

### *2.2. Isolation of cultivable bacterial pyrene degraders, and pyrene degradation experiment in pure culture*

Four grams of original soils were added into 100 mL of enrichment medium (details in Supporting Information) supplemented with pyrene (100 mg/L, details in Supporting Information). After 7-day incubation with continuous shaking (180 rpm) at 28°C in the dark, 1 mL of the suspension was transferred into 100 mL of fresh enrichment medium with increasing pyrene concentration (200, 300, 400 and 500 mg/L). Afterwards, the

enriched suspension was diluted and spread onto a mineral medium agar plate supplemented with pyrene (500 mg/L, Supporting Information) as the sole carbon source (Zhang, et al., 2012). After incubation at 28°C for 2 days in the dark, single colonies were picked from the plate and streaked twice on fresh mineral medium agar plates supplemented with pyrene (500 mg/L). Then the 16S rRNA of all the isolates were sequenced, and compared to that in NCBI database.

The isolated pyrene-degrading strain were pre-cultured in 10 mL minimal medium (containing 500 mg/L pyrene) at 28 °C for 24 h, shaking at 180 rpm. When the cells reached the logarithmic phase with an OD 600 of 0.5-0.6, they were washed twice at 4000 rcf for 10 min and resuspended in fresh minimal media. Subsequently, the resuspended cells were transferred to 100 mL minimal medium containing 500 mg/L pyrene for further study on pyrene degradation in pure culture.

### 2.3. *Pyrene degradation microcosms*

To enrich active pyrene degraders and explore pyrene biodegradation performance in soils, five treatments were carried out. The sterile control (OS\_CK) was prepared by sterilizing the soils with HgCl<sub>2</sub> (0.1%) and supplemented with pyrene to study abiotic pyrene degradation. As bioaugmentation is normally applied to original soils by adding target degraders, we followed the same principle to use original soils for bioaugmentation treatments. Generally, treatments with original soils were named as 'OS\_', treatments with soils functionalized with MNP were designated as 'MMI\_', and bioaugmentation treatments were named as 'BA\_'. The four biotic treatments included original soils without pyrene (OS\_NC), original soils supplemented with pyrene (OS\_Pyr), MNP-functionalized soils without pyrene (MMI\_NC) and MNP-functionalized soils supplemented with pyrene (MMI\_Pyr).

MNPs synthesis followed our published method (Zhang, et al., 2011) and the concentration was 9.1 g/L. To functionalize soils, 0.91 mg of synthesized MNPs (0.1 mL) were added to 500 mg soils (dry weight) according to the optimal dosage for soil magnetic functionalization (Wang, et al., 2016a). For OS\_CK, OS\_Pyr and MMI\_Pyr treatments, pyrene was set at a final concentration of 100 mg/kg, meeting with the average contamination level at the contaminated site. Each treatment was conducted in triplicates and incubated at room temperature for 30 days. After 0, 10, 20 and 30 days of cultivation, 5.0 g of soil samples were collected for chemical analysis and DNA extraction. To separate the active pyrene degrading consortium (magnetic-free cells, MFCs), 2.0 g of soils were collected from MMI\_NC and MMI\_Pyr treatments on Day 0, 10, 20 and 30. Subsequently, the soils were added with 3 mL of soil extraction solution (2.0 g of original soils with 20 mL deionized water and passing through a 0.45-mm filter) and further separated by a permanent magnet (Li, et al., 2018b). MFCs in suspensions separated from MMI\_NC and MMI\_Pyr treatment were designated as MFC\_NC and MFC\_Pyr.

Bioaugmentation experiment introduced the cultivable pyrene degrader *Sphingomonas* sp. YT1005 or MFCs (MMI-enriched pyrene-degrading consortium) into soils with total populations of  $10^9$  cells/g soil. The four treatments included: original soils supplemented with the cultivable pyrene degrader (*Sphingomonas* sp. YT1005) was represented as BA\_Sph, and sterile soils (treated with UV-254 for 30 min) supplemented with the cultivable pyrene degrader (*Sphingomonas* sp. YT1005) was represented as CK\_Sph, original soils supplemented with MFCs was represented as BA\_MFC, and sterile soils (treated with UV-254 for 30 min) supplemented with MFCs was represented as CK\_MFC. Pyrene was set at a final concentration of 100 mg/kg in

all treatments, which were incubated at 28°C in the dark in triplicates. Finally, 5.0 g of soils were sacrificed after 0, 10 and 20 days for chemical analysis and DNA extraction.

#### 2.4. DNA extraction, quantification, sequence and analysis

Soil genomic DNA was extracted from all 19 soil samples in all treatments using a MO BIO PowerSoil DNA Isolation Kit (MoBio Laboratories, Inc., USA) according to the manufacturer's instructions. DNA concentration was determined by spectrophotometry (NanoDrop 2000, Wilmington, DE). Quantitative PCR (qPCR) was performed for the abundance of bacterial 16S rRNA and pyrene dioxygenase encoding genes (Cebren, et al., 2008, Zhou, et al., 2006), including PAH-RHD $\alpha$ -GP, PAH-RHD $\alpha$ -GN, *nidA* and *nidA3* (in Table S3). The 20  $\mu$ L qPCR system consisted of 2  $\mu$ L of each primer, 1  $\mu$ L of DNA template, 5  $\mu$ L of ultrapure water and 10  $\mu$ L of iTaq™ Universal SYBR® Green Supermix (BioRad, USA). Standard curves were obtained with serial dilutions of quantified plasmid DNA containing the fragment of 16S rRNA and pyrene-degrading genes (Jiang, et al., 2019). The primer and qPCR programs were listed in Table S3.

To assess bacterial community composition and diversity, the extracted DNA was amplified and sequenced targeting the V3-V4 regions of 16S rRNA genes (Sangon Biotech Co., Ltd, Beijing, China). PCR was performed using the universal primer set of 515F (5'-GTGCCAGCMGCCGCGGTAA-3') and 806R (5'-GGACTACHVGGGTWTCTAAT-3') (Song, et al., 2015). Sequencing was performed by Illumina Miseq™ and all sequence reads were quality checked after removing primer connector sequences, merging paired reads and distinguishing samples according to barcodes (NCBI BioProject ID: PRJNA534380). Sequences were classified as operational taxonomic units (OTUs) with 97% similarity and then assigned by Ribosomal Database Project (RDP) classifier based on Bergey's

taxonomy. Bacterial alpha-diversity indices (Chao1, Shannon and Simpson) were analyzed by QIIME (v1.80) to assess bacterial species richness and diversity. The distance matrices from samples were generated by the Bray-Curtis metric and visualized by principal coordinates analysis (PCoA) by QIIME (Quantitative Insights Into Microbial Ecology) software (Wang, et al., 2016a).

### 2.5. Chemical analysis

To analyze soil pyrene contents, 5.0 g of soils were blended with 3 g of anhydrous  $\text{Na}_2\text{SO}_4$ , spiked with 10 mL of surrogate standards (10  $\mu\text{g}/\text{mL}$ , phenanthrene-d10, AccuStandard<sup>®</sup>, Inc.), and added with 15 mL of extraction solvent (hexane:acetone=1:1, v/v). After ultrasonication-assisted extraction for 20 min, the suspension was centrifuged for 3 min at 15,000 rcf. The extraction process was repeated twice, and the three fractions of supernatants were mixed and concentrated using a rotary evaporator to a final volume of approximately 2 mL at 60°C. It was further purified by solid phase extraction cartridges (Bond Elut-C18, 100 mg/1 mL, Agilent), which were pre-conditioned with 4 mL of dichloromethane and 10 mL of hexane, and washed by 5 mL of dichloromethane:hexane (1:9, v/v). After soaking for 2 min, another 5 mL of dichloromethane:hexane (1:9, v/v) were added to elute pyrene and the filtrates were concentrated to completely dry under a gentle stream of nitrogen gas. Internal standards (fluorene, 100  $\mu\text{g}/\text{mL}$ ) were added to each filtrate prior to instrumental analysis.

The quantitative analysis of pyrene was performed using a gas chromatography mass spectrometry (GC-MS, Shimadzu, QP2010SE) equipped with a DB-5MS capillary column (30 m in length, 0.25 mm in diameter, 0.25  $\mu\text{m}$  thickness) and a mass spectrometric detector (ionisation energy, 70 eV, details in Supporting Information).

Five pyrene standard concentrations (5-500 ng/mL) were used to derive the calibration curve for pyrene ( $R^2 > 0.999$ ). Mean recoveries of surrogate standards (phenanthrene-d10) in the present study ranged from 90% to 105% and the final concentrations of pyrene were corrected by surrogate recovery. For the detection of PAH metabolites, the samples were derivatized with BSTFA/TMCS (99:1) (bis(trimethylsilyl) trifluoroacetamide N trimethylchlorosilane) for 1 h at 68°C, and then detected with GC-MS as previously reported (Lu, et al., 2013, Wu, et al., 2019). The details for PAHs metabolite detection were provided in Supporting Information. The molecular mass of each metabolite was searched against previous literatures and the database of PAH metabolites (National Institute of Standards and Technology, NIST). The chemical structure of each possible metabolite was confirmed by the pattern of fragment ions in the mass spectrum.

## 2.6. Statistical analysis

Statistical analysis was performed by SPSS 20.0 software. One-way analysis of variance (ANOVA) was used to compare the difference in pyrene contents and the relative abundance of 16S rRNA and pyrene dioxygenase encoding genes ( $p < 0.05$ ). The correlation matrix was calculated and visualized using R (version 3.5.3). The phylogenetic tree of 16S rRNA genes was constructed according to the neighbor joining method using Molecular Evolutionary Genetics Analysis (MEGA). Molecular ecological network was constructed by online MENA (Molecular Ecological Network Analyses) pipeline (<http://ieg2.ou.edu/MENA>) using Spearman's Rho with default parameters (Deng, et al., 2018).

The logarithmic nonlinear regression between pyrene degradation efficiency ( $P_D$ , %) and the abundance of pyrene dioxygenase encoding genes ( $Pyrene_g$ , copies/g soil) followed Equation (1):

$$P_D = P_0 + a \times \ln(Pyrene_g) \quad (1)$$

Here,  $P_0$  and  $a$  represents pyrene degradation efficiency in abiotic treatments and correlation slope, respectively.

### 3. Results

#### 3.1. Biodegradation and bioaugmentation performance

Pyrene degradation efficiencies in different treatments are illustrated in Figure 1. In abiotic treatment (OS\_CK), pyrene content did not show significant decrease throughout the incubation period. An acceptable pyrene degradation was achieved in OS\_Pyr treatment, and pyrene degradation efficiency was 30.18% on day 10 and 44.24% on day 20.

After introducing the cultivable pyrene degraders (*Sphingomonas* sp. YT1005 in BA\_Sph and CK\_Sph treatments and MMI-isolated active pyrene-degrading consortium in BA\_MFC and CK\_MFC treatments) in bioaugmentation, pyrene degradation performance varied remarkably across treatments (Figure 1). An unexpected postpone of pyrene degradation was found in BA\_Sph and CK\_Sph treatments that pyrene degradation efficiency was less than 20% after 20-day incubation, exhibiting no significant difference with that in abiotic sterile treatment (OS\_CK,  $p > 0.05$ ). BA\_MFC treatment (original soils with MMI-isolated active pyrene-degrading consortium) accelerated pyrene degradation efficiency to 57.79% on

day 10 and 74.41% on day 20. It is worth highlighting that CK\_MFC treatment (sterile soils with MMI-isolated active pyrene-degrading consortium) had a similar pyrene degradation curve as OS\_Pyr treatment, suggesting that the introduced active pyrene-degrading consortium alone had the same pyrene degradation capabilities as indigenous soil microbes.

Both first-order and second-order pyrene degradation kinetics were calculated for the five treatments, including OS\_Pyr, BA\_Sph, CK\_Sph, BA\_MFC and CK\_MFC. Except for pyrene degradation in BA\_Sph treatment as a second-order kinetics with a half-life ( $t_{1/2}$ ) of 14.28 d ( $R^2=0.5895$ ), other pyrene degradation processes all followed the first-order kinetics, and  $t_{1/2}$  was 9.49 (OS\_Pyr,  $R^2=0.7656$ ), 10.50 (CK\_Sph,  $R^2=0.6515$ ), 6.99 (BA\_MFC,  $R^2=0.9108$ ) and 7.89 d (CK\_MFC,  $R^2=0.7673$ ). This result indicated that bioaugmentation with the active pyrene degraders (BA\_MFC and CK\_MFC) could significantly accelerate pyrene biodegradation.

### *3.2. Microbial community diversity and structure during pyrene degradation process*

After processing raw data obtained by Illumina Miseq, a total of 895,290 raw reads with a length of >450 bp were obtained from 19 soil samples in five treatments, ranging from 50,899 in MMI\_Pyr\_30 to 77,369 in MMI\_Pyr\_20. They were assigned into 15,210 OTUs affiliated with 30 bacterial phyla and 100 bacterial genera. Across all samples, the Good's coverage ranged from 0.95 to 0.99, indicating a satisfactory coverage of bacterial lineages for further analysis. In all treatments, bacterial alpha-diversity indices (Chao1, Shannon and Simpson) did not show significant difference (Table S4).

*Sphingomonas* was the most predominant bacterial genus, accounting for 4.12% of total bacterial populations in treatment without pyrene (OS\_NC) to 37.81% in MFC\_Pyr treatments. Other dominant bacterial genera included *Arthrobacter* (9.33% to 9.87%), *Lysobacter* (3.42% to 6.24%), *Rhodococcus* (3.07% to 5.19%), *Pedobacter* (3.43% to 4.06%), *Aeromicrobium* (3.00% to 3.07%) and *Pseudonocardia* (2.47% to 3.58%) in original soils and OS\_NC treatments (Figure S1).

From bacterial beta-diversity distance matrices (Figure 2A), bacterial community compositions in OS\_NC and OS\_Pyr treatments were similar and clustered together in the first 10-day of pyrene degradation. Afterwards, the relative abundance of some bacterial taxa in OS\_Pyr treatments was significantly higher than that in OS\_NC treatments, including *Kribbella* (2.00%), *Streptomyces* (2.92%), *Lysobacter* (8.69%), *Streptomyces* (4.75%) and *Thermomonas* (3.24%). Accordingly, the groups of OS\_NC and OS\_Pyr were separated after day 10. Similarly, bacterial communities in MMI\_NC and MMI\_Pyr treatments were also clustered (Figure 2A). In the absence of pyrene, bacterial community composition showed no difference between MMI\_NC and MFC\_NC (Figure 2B).

### 3.3. Pyrene degraders revealed by cultivation-dependent and cultivation-independent methods

In total, 8 isolates were obtained from mineral medium agar plates supplemented with pyrene. The results of 16S rRNA gene sequencing demonstrated that all isolates have identical sequence, exhibiting 98% similarity with *Sphingomonas echinoides* DSM 1805 (NCBI Accession No: MK934417). This cultivable pyrene degrader was then designated as *Sphingomonas* sp. YT1005 (amplification and sequence details in Supporting Information, NCBI Accession No. MK934417.1). With pyrene as the sole

carbon source, this strain formed orange pigmented colonies on agar plates. Additionally, *Sphingomonas* sp. YT1005 had a satisfactory pyrene degradation efficiency, which achieved 62.3% after 10-day incubation in mineral medium.

In treatments with MNPs functionalized bacteria (MMI\_Pyr treatment), the active pyrene degraders could utilize pyrene and proliferate, gradually losing MNPs on the membrane of the newly-formed pyrene degrading cells. In contrast, all the other inert cells maintained their magnetism and could be separated by external magnetic field (Wang, et al., 2016a, Zhang, et al., 2011, Zhang, et al., 2015). Bacterial beta-diversity distance matrices illustrated that MFCs isolated from MMI\_Pyr treatment (MFC\_Pyr) were separated from the whole community in MMI\_Pyr treatment and MFC\_NC (MFCs from MMI\_NC treatments, Figure 2B). Accordingly, by comparing the relative abundance of bacterial lineages, several bacterial genera were much higher in MFC\_Pyr and they were potentially the active pyrene degraders. They included *Gp16*, *Streptomyces*, *Pseudonocardia*, *Panacagrimonas*, *Methylotenera* and *Nitrospira*, which was  $1.442 \pm 0.207$ ,  $1.511 \pm 0.216$ ,  $1.621 \pm 0.615$ ,  $4.573 \pm 1.641$ ,  $2.526 \pm 0.698$  and  $1.533 \pm 0.052$  times more enriched in MFC\_Pyr, respectively (Figure 2C).

In treatments without pyrene (OS\_NC), neither *Sphingomonas* sp. YT1005 nor the active pyrene degrading consortium (*Gp16*, *Streptomyces*, *Pseudonocardia*, *Panacagrimonas*, *Methylotenera* and *Nitrospira*) were enriched in the magnetic-free fraction (MFC\_NC, Figure 3A), remaining 28.0-30.6% and 1.9-3.0% throughout the pyrene degradation process, respectively. In contrast, the relative abundance of *Sphingomonas* sp. YT1005 in MFC\_Pyr fraction significantly decreased from 26.5% to 8.5%, whereas the relative abundance of the potential pyrene degraders increased from 2.3% to 5.2% (Figure 3B).

The phylogenetic tree of the cultivable pyrene degrader *Sphingomonas* sp. YT1005 and the potential active pyrene degraders in MFC\_Pyr was illustrated in Figure 3C. *Sphingomonas* sp. YT1005 is clustered with other *Sphingomonas* species, e.g., *Sphingomonas echinoides* and *Sphingomonas glacialis*. All the potential active pyrene degraders isolated from MMI\_Pyr treatment, including *Nitrospira* (OTU23472), *Gp16* (OTU33542), *Streptomyces* (OTU29458), *Pseudonocardia* (OTU29851), *Panacagrimonas* (OTU4395) and *Methylotenera* (OTU583), were clustered in a separate branch.

### 3.4. Intra-correlation within soil bacterial community

To explain the mechanisms of bioaugmentation postpone in BA\_Sph and CK\_Sph treatments, we analyzed the bacterial intra-correlations by molecular ecological network (Figure 4, Table S5). The results suggested a complex microbial network in soils (avgK=4.356 and avgCC=0.205), including 4 major modules, 360 nodes and 784 significant correlations ( $p < 0.01$ ). The majority (90.1%) of the correlations were positive, and the cultivable pyrene degrader *Sphingomonas* (OTU33525) exhibited 12 positive links with Module 2. Four of the potential active pyrene degraders (*Nitrospira*, OTU23472; *Streptomyces*, OTU29458; *Panacagrimonas*, OTU4395; *Methylotenera* OTU583) had 39 correlations with other bacterial lineages, 56.4% of which were negative. It is worth noting that, although there was no direct correlation between the cultivable pyrene degrader *Sphingomonas* and the potential active pyrene degraders, 11 indirect correlations (mediated by other microbes from the 4 major modules) were observed and they were all negative. Additionally, Mantel test confirmed the negative correlations between *Sphingomonas* and the potential active pyrene degraders ( $p < 0.05$ ), and the correlation coefficient was -0.7285 for *Gp16*, -0.7533 for *Streptomyces*,

-0.8287 for *Pseudonocardia*, -0.7548 for *Panacagrimonas* and -0.7956 for *Methylotenera* ( $p < 0.05$ ). Our results therefore uncovered negative correlations between the cultivable pyrene degrader *Sphingomonas* sp. YT1005 and the active pyrene degrading consortium isolated by MMI, which suppressed the bioaugmentation performance at the beginning in BA\_Sph and CK\_Sph treatments.

### 3.5. Dynamics of pyrene dioxygenase encoding genes

No PAH-RHD $\alpha$ -GN gene was successfully amplified in any treatment. The relative abundance of *nidA*, *nidA3*, and PAH-RHD $\alpha$ -GP genes in OS\_NC treatment remained constant throughout the incubation period (Figure 5A), ranging from  $0.96 \times 10^{-7}$  to  $1.32 \times 10^{-7}$ ,  $3.62 \times 10^{-7}$  to  $4.25 \times 10^{-7}$  and  $44.5 \times 10^{-7}$  to  $50.1 \times 10^{-7}$ , respectively. It indicated a neglectable increase of pyrene dioxygenase encoding genes in the absence of pyrene. The relative abundance of *nidA*, *nidA3* and PAH-RHD $\alpha$ -GP genes increased significantly ( $p < 0.01$ ) in OS\_Pyr treatments since day 20 and finally achieved  $1.00 \times 10^{-5}$ ,  $2.84 \times 10^{-5}$  and  $2.15 \times 10^{-5}$  on day 30, which was 105.5, 74.6 and 4.7 times higher than those in OS\_NC treatments. Interestingly, all these pyrene dioxygenase encoding genes dramatically increased in MFC\_Pyr from day 10. After 30-day degradation, the relative abundance of *nidA*, *nidA3* and PAH-RHD $\alpha$ -GP genes increased to  $1.13 \times 10^{-4}$ ,  $2.88 \times 10^{-4}$  and  $2.24 \times 10^{-4}$ , which was 1182.6, 754.8 and 49.3 times higher than that in OS\_NC treatments.

There were significantly positive correlations between pyrene degradation efficiency and the relative abundance of *nidA*, *nidA3* and PAH-RHD $\alpha$ -GP genes ( $p < 0.01$ , Table S6). The regression coefficient was  $2.72 \times 10^{-6}$  ( $r^2 = 0.9671$ ),  $4.74 \times 10^{-6}$  ( $r^2 = 0.9064$ ) and  $1.60 \times 10^{-6}$  ( $r^2 = 0.8790$ ) for *nidA*, *nidA3* and PAH-RHD $\alpha$  GP genes, respectively (Figure 5D).

The abundance of the active pyrene degraders in MFC\_pyr increased during the degradation process from 2.3% (Day 10) to 5.2% (Day 30, Figure 3B), 1.74- and 2.26-times higher on Day 20 and Day 30, respectively. The relative abundance of pyrene-degrading genes in MFC\_pyr treatment also increased (Figure 5C). For instance, the relative abundance of *nidA* gene was  $3.68 \times 10^{-5}$ ,  $3.71 \times 10^{-5}$  and  $1.13 \times 10^{-4}$  on Day 10, 20 and 30, respectively. The relative abundance of *nidA3* and PAH-RHD $\alpha$ -GP genes was 3.88- and 2.60-times higher on Day 30 than those on Day 10. The similar increasing trends of the active pyrene degraders (Figure 3B) and pyrene-degrading genes (Figure 5) hinted that these active pyrene degraders harbor the studied pyrene-degrading genes for pyrene metabolism.

### 3.6. Metabolites and degradation pathway of pyrene

To understand pyrene degradation pathways in bioaugmentation, metabolites were analyzed during pyrene biodegradation process in CK\_Sph and CK\_MFC treatments. In total, ten metabolites were identified, and two pyrene degradation pathways were proposed (Figure 6 and S3, Table S7).

In CK\_Sph treatment, the metabolite *cis*-4,5-pyrene dihydrodiol ( $m/z=364$ ,  $t_R=19.82$  min) might be generated from an initial pyrene oxidation at C-4 and C-5 positions by dioxygenase, designated as metabolite ①. Although the following metabolite phenanthrene-4-carboxylic acid (by *ortho*-cleavage and decarboxylation) was not detectable, its downstream metabolite was detected as dihydroxyphenanthrene (metabolite ②,  $m/z=355$ ,  $t_R=5.31$  min). Further oxidation of dihydroxyphenanthrene generated 2-hydroxy-2-H-benzo[h]chromene-2-carboxylic acid (metabolite ③,  $m/z=415$ ) by extradiol dioxygenase after ring cleavage, and subsequent to

2-methylnaphthalene (metabolite ④,  $m/z=142$ ) and 1-hydroxy-2-naphthoic acid (metabolite ⑤,  $m/z=202$ ). Finally, metabolite ⑥ ( $m/z=167$ ,  $t_R=21.73$  min) was identified as phthalic acid comparing to the mass spectral library (NIST). From these metabolites, there was only one phthalate pathway by the cultivable pyrene degrader *Sphingomonas* sp. YT1005.

In CK\_MFC treatments, all ten metabolites are identified (Figure 6 and S3, Table S7). Besides those in the phthalate pathway in CK\_Sph treatment, metabolite ⑦ ( $m/z=427$ ) was protocatechuic acid, a downstream metabolite of phthalic acid by dioxygenase, dehydrogenase and decarboxylase. It suggested that phthalic acid was further metabolized by the active pyrene degrading consortium enriched by MMI and entered the tricarboxylic acid (TCA) cycle via  $\beta$ -keto adipate pathway. Alternatively, metabolite ⑧ ( $m/z=267$ ) was identified as 4-phenanthrenol from phenanthrene-4-carboxylic acid. Metabolite ⑨ ( $m/z=206$ ,  $t_R=8.47$  min) and metabolite ⑩ ( $m/z=206$ ,  $t_R=20.87$  min) was *trans*-2'-carboxybenzalpyruvate and salicylic acid, respectively. They were two downstream metabolites of 1-hydroxy-2-naphthoic acid (metabolite ⑤). As metabolites ⑨ and ⑩ were only detectable in CK\_MFC treatment, MMI-enriched active pyrene degrading consortium exhibited a unique salicylate pathway for pyrene degradation.

In the phthalate pathway, metabolites ①, ②, ③ and ④ were detected in all treatments but only on Day 10. Metabolite ⑤ was detected on all sampling days in all treatments, whereas metabolites ⑥ was only detectable on Day 20. These results suggested metabolites ①, ②, ③ and ④ were gradually metabolized into downstream metabolites (⑤ and ⑥), which accumulated during pyrene degradation

process. In the salicylate pathway, metabolite ⑧ was detected on days 20 and 30, also suggesting a significant accumulation of downstream metabolites.

#### 4. Discussion

Pyrene is a typical PAH for its similar structure to several carcinogenic PAHs (Peng, et al., 2008). Pyrene biodegradation has been intensively studied, either as carbon and energy source, or as a non-growth substrate in co-metabolism (Johnsen, et al., 2005, Nzila, 2013). Pyrene degraders include *Acinetobacter* (Jiang, et al., 2018b), *Burkholderia* (Vaidya, et al., 2017), *Bacillus* (Rabodonirina, et al., 2018), *Mycobacterium* (Wu, et al., 2019), *Pseudomonas* (Khan, et al., 2018), *Rhodococcus* (Jia, et al., 2019) and *Sphingomonas* (Guo, et al., 2017). In the present study, *Sphingomonas* sp. YT1005 was identified as a cultivable pyrene degrader from soils at an abandoned steel plant site. *Sphingomonas* is a typical PAH-degrading microorganism (Zhao, et al., 2017). *Sphingomonas* LB126 is reported to use fluorene as the sole carbon or energy source and can co-metabolize phenanthrene, fluoranthene, anthracene and dibenzothiophene (van Herwijnen, et al., 2003). *Sphingomonas* sp. GY2B isolated from petroleum-contaminated soils could degrade phenanthrene through the salicylate pathway (Tao, et al., 2007). However, the isolated strain *Sphingomonas* sp. YT1005 in this study was affiliated close to *Sphingomonas echinoides*, which is not previously linked with pyrene degradation, and our study brought direct evidence of their functions in metabolizing pyrene.

The dominant bacterial genera in soils (*Sphingomonas*, *Arthrobacter*, *Lysobacter*, *Rhodococcus*, *Pedobacter*, *Aeromicrobium* and *Pseudonocardia*) are abundant soil bacterial lineages (Delgado-Baquerizo, et al., 2018) and participate in soil carbon and nitrogen cycles (Schimel and Schaeffer, 2012). After pyrene degradation, the relative

abundance of *Pseudonocardia*, *Streptomyces*, *Lysobacter* and *Thermomonas* significantly increased. They are reported to be responsible for PAHs biodegradation by many previous studies. *Lysobacter* is linked to pyrene degradation (Wang, et al., 2018) and *Thermomonas* has the capacity of degrading anthracene (Nzila, et al., 2018). Our findings were consistent with these reports and indicated that predominant bacterial taxa in pyrene-contaminated soils were related to pyrene tolerance or degradation.

Both bacterial  $\alpha$ -diversity and community composition were of no significant difference between OS\_NC and MMI\_NC treatments, indicating that MNP-functionalization had little impacts on soil bacterial community and did not affect pyrene biodegradation process (Wang, et al., 2016a). During the pyrene degradation process, the active pyrene degraders utilized pyrene and lost magnetism gradually, resulting in their enrichment in the magnetic-free fractions of MFCs (Zhang, et al., 2015). Accordingly, the community structure of MFC\_Pyr was different from MFC\_NC and the enriched bacterial lineages were the potential active pyrene degraders (Figure 2B).

The active pyrene degrading consortium isolated by MMI included *Gp16*, *Streptomyces*, *Pseudonocardia*, *Panacagrimonas*, *Methylotenera* and *Nitrospira* (Figure 3C). Among them, the roles of *Streptomyces* and *Pseudonocardia* in PAH biodegradation have been previously reported (Chaudhary, et al., 2011, Chen, et al., 2018). *Pseudonocardia* could degrade pyrene in agricultural soils (Chen, et al., 2018) and *Streptomyces rochei* was capable of using anthracene, fluorene, phenanthrene and pyrene as the sole carbon source (Chaudhary, et al., 2011). As for other bacterial taxa, *Gp16* is reported to tolerate toxic chemicals (De, et al., 2003, De and Ramaiah, 2007), and *Methylotenera* is a methylamine- and methanol-utilizing bacterium with denitrification capability (Kalyuzhnaya, et al., 2010, Mustakhimov, et al., 2013).

*Panacagrimonas* is newly isolated from soils (Im, et al., 2010) and enriched in the rhizosphere of pioneer plants in metal-contaminated soils (Navarro-Noya, et al., 2010). *Nitrospira* is normally viewed as key nitrifiers in soils (Li, et al., 2019, Wang, et al., 2019). However, no study has ever reported their involvement in pyrene degradation, and this work broadened our understanding on pyrene-degrading microbes, suggesting that numerous soil microbes have the capability to degrade pyrene.

The relative abundance of all pyrene dioxygenase genes was higher in OS\_Pyr than OS\_NC treatments, hinting the enrichment of pyrene degraders harboring dioxygenase genes with pyrene amendment. Additionally, their relative abundance was around 10-200 folds higher in MFC\_Pyr than OS\_Pyr, proving the successful isolation of the active pyrene degrading microbes in MFC fractions (Figure 5A). Each pyrene dioxygenase gene exhibited a positive correlation with pyrene degradation efficiency (Figure 5 and Table S6), suggesting their critical roles in pyrene degradation. *nidA*, *nidA3* and PAH-RHD $\alpha$ -GP genes are reported as biomarkers for pyrene degradation in many previous studies. As a key gene for the initial hydroxylation of PAH aromatic ring, the  $\alpha$  subunit of *nidA*-encoding dioxygenase was cloned in *Mycobacterium* sp. strain PYR-1 (Hall, et al., 2005, Khan, et al., 2001) and proved to be critical in pyrene degradation (Guo, et al., 2010). The relative abundance of *nidA3* gene was linked to pyrene biodegradation efficiency by PAH-degrading communities (Chen, et al., 2016). PAH-RHD $\alpha$ -GP genes in the initial step of PAH aerobic metabolism demonstrated a positive correlation with PAH biodegradation potential in soils (Cebren, et al., 2008, Jurelevicius, et al., 2012). In addition, the relative abundance of all pyrene dioxygenase genes was also positively correlated with that of the potential active pyrene degraders in MFC\_Pyr treatment (0.8611,  $p < 0.01$ ), hinting that they might harbor these pyrene dioxygenase encoding genes.

Cultivable pyrene degrader *Sphingomonas* sp. YT1005 was found to degrade pyrene following the phthalate pathway. All the metabolites in CK\_Sph treatments have been reported as key metabolites in the phthalate pathway by previous studies, *e.g.*, *cis*-4,5-pyrene dihydrodiol (metabolite ①) (Luan, et al., 2006, Zhong, et al., 2006), dihydroxyphenanthrene (metabolite ②) (Beaubien, 2020), 2-hydroxy-2-H-benzo[h]chromene-2-carboxylic acid (metabolite ③) (Wu, et al., 2019, Zhou, et al., 2016), 2-methylnaphthalene (metabolite ④) (Wu, et al., 2019) and 1-hydroxy-2-naphthoic acid (metabolite ⑤). In contrast, metabolites of protocatechuic acid (metabolite ⑦) (Jin, et al., 2016a), 4-phenanthrenol (metabolite ⑧) (Beaubien, 2020, Wu, et al., 2019), *trans*-2'-carboxybenzalpyruvate (metabolite ⑨) and salicylic acid (metabolite ⑩) (Zhong, et al., 2017, Zhou, et al., 2016) are involved in the salicylate pathway of PAHs degradation. Thus, MMI-isolated pyrene degrading consortium metabolized pyrene through both phthalate and salicylate pathways (Figure 6). Both phthalate and salicylate pathways are important in pyrene metabolism (Sun, et al., 2019) and previously reported for the degradation of other PAHs. Pyrene-degrading strains mainly exhibit the phthalate pathway for pyrene (Jin, et al., 2016b, Liang, et al., 2006). Only few studies suggested the involvement of salicylate pathway in pyrene degradation, such as *Mycobacterium* sp. WY10 which degrades pyrene predominantly in the phthalate pathway and minorly in the salicylate pathway (Sun, et al., 2019). The extra salicylate pathway imposed by MMI-isolated pyrene degrading consortium suggested a more complex pyrene degradation pathways in natural habitats than individual pyrene-degrading strains (Gallego, et al., 2014, Zafra, et al., 2017), hinting a underestimated diversity of pyrene degraders. MMI is therefore an effective approach to separate the active pyrene degraders from soil

matrices, not only helping in building up high-efficient degrading consortiums for bioaugmentation but also contributing to our deeper understanding on the actual players and pathways for pyrene metabolism in soils.

Enhanced pyrene degradation performance by bioaugmentation with soil indigenous microbes has been reported in many previous studies (Chen, et al., 2016, Wang, et al., 2018). However, bioaugmentation postpone or even failure commonly occurs, generally explained by microbial acclimation to environment changes, *e.g.*, morphological, physiological and behavioral adjustments (Macleod and Semple, 2006, Ren, et al., 2018). In the present study, bioaugmentation with *Sphingomonas* sp. YT1005 in either sterile (CK\_Sph) or original soils (BA\_Sph) did not achieve satisfactory pyrene degradation performance at the initial stage (0-20 days, Figure 1). This result suggested that *Sphingomonas* sp. YT1005 was a cultivable pyrene degrader in artificial medium and did not exhibit significant pyrene degradation ability in ambient soils. In addition, the consistent pyrene degradation efficiency in OS\_Pyr and CK\_MFC treatments proved that MMI-enriched bacterial consortiums consisting of *Gp16*, *Streptomyces*, *Pseudonocardia*, *Panacagrimonas*, *Methylotenera* and *Nitrospira* were the actual pyrene degraders responsible for *in-situ* pyrene metabolism. The half-life ( $t_{1/2}$ ) of pyrene in bioaugmentation with the active pyrene degrading consortium (6.99-7.89 d) was significantly shorter than previous reports (10-59 d) (Kashyap and Moholkar, 2021, Obayori, et al., 2017, Ukalska-Jaruga, et al., 2020), indicating the potential to use MMI-enriched consortium for enhanced bioremediation. We found negative intra-correlations between *Sphingomonas* sp. YT1005 and the active pyrene degraders from the co-occurrence molecular ecological network (Figure 4), and also observed their opposite trends during the pyrene degradation process

(Figure 3B), possibly explaining the postponed pyrene degradation in CK\_Sph and BA\_Sph treatments at the beginning stage of bioaugmentation.

A further insight into correlation network of *Sphingomonas* sp. YT1005 and the active pyrene degraders (Figure S2) demonstrated that the introduction of *Sphingomonas* sp. in BA\_Sph treatments therefore inhibited their activities and consequently resulted in bioaugmentation postpone, attributing to the complex bacterial intra-correlations within the bacterial community. This explanation was consistent with some previous studies that the correlation between pure-cultivation isolated and indigenous degraders affected the bioaugmentation performance. Non-active degrader *Marmoricola* LJ-33 significantly enhanced biphenyl degradation efficiency in soils by changing bacterial diversity in biphenyl metabolism (Tang, et al., 2020). Another bioaugmentation by PAH-degrader *Acinetobacter tandoii* LJ-5 produced a significant increased phenanthrene mineralization, attributing to the altered diversity of the active phenanthrene degraders, instead of *Acinetobacter tandoii* LJ-5 itself (Li, et al., 2018a). We then propose the mechanism explaining bioaugmentation performance regarding intra-correlations between cultivable and active pyrene degraders. Enhanced bioaugmentation is expected when these two groups of bacteria exhibit positive intra-correlations, whereas negative intra-correlations between cultivable and active pyrene degraders consequently result in bioaugmentation postpone or failure. As for neutral intra-correlations, the effectiveness and performance of bioaugmentation is non-deterministic and potentially dependent on other environmental variables.

## 5. Conclusions

This study investigated soil pyrene degraders via both cultivation-dependent and cultivation-independent approaches. *Sphingomonas* sp. YT1005 was isolated via pure cultivation, and the active pyrene degrading consortium consisting of *Gp16*, *Streptomyces*, *Pseudonocardia*, *Panacagrimonas*, *Methylotenera* and *Nitrospira* was isolated by MMI. An unexpected postpone of pyrene degradation was found in bioaugmentation with *Sphingomonas* sp. YT1005, explained by its negative intra-correlations with the active pyrene degraders. In contrast, bioaugmentation with MMI-isolated pyrene degrading consortium significantly accelerated pyrene degradation in soils. It was supported by the increasing relative abundance of pyrene dioxygenase encoding genes (*nidA*, *nidA3* and PAH-RHD $\alpha$ -GP) along with pyrene degradation efficiency. Further analysis of pyrene degradation pathway suggested that *Sphingomonas* sp. YT1005 only exhibited the phthalate pathway, whereas MMI-isolated pyrene degraders possessed both phthalate and salicylate pathways. This work broadens our vision on the actual pyrene degradation process and mechanisms in soils, suggesting that intra-correlations between the introduced degraders and the indigenous active degraders are key factors determining bioaugmentation performance. Isolating and reintroducing the active indigenous active degraders is a more promising strategy for bioaugmentation.

## 6. Acknowledgments

Financial support was provided by the National Natural Science Foundation of China (41807119), the Natural Science Foundation of Beijing, China (8212030), Special Fund of State Key Joint Laboratory of Environment Simulation and Pollution Control

(19K04ESPCT), Fundamental Research Funds for the Central Universities (FRF-TP-20-010A3), the Open Fund of National Engineering Laboratory for Site Remediation Technologies (NEL-SRT201907), and Beijing Municipal Science and Technology Project (Z181100002418016). DZ also acknowledges the support of Chinese Government's Thousand Talents Plan for Young Professionals.

## 7. References

- [1] Beaubien, J., 2020. How South Korea Reined In The Outbreak Without Shutting Everything Down, Goats and Soda : NPR.
- [2] Bosch, R., Garcia-Valdes, E., Moore, E.R.B., 2000. Complete nucleotide sequence and evolutionary significance of a chromosomally encoded naphthalene-degradation lower pathway from *Pseudomonas stutzeri* AN10, Gene 245, 65-74.
- [3] Cebren, A., Norini, M.-P., Beguiristain, T., Leyval, C., 2008. Real-Time PCR quantification of PAH-ring hydroxylating dioxygenase (PAH-RHD alpha) genes from Gram positive and Gram negative bacteria in soil and sediment samples, *Journal of microbiological methods* 73, 148-159.
- [4] Chaudhary, P., Sharma, R., Singh, S.B., Nain, L., 2011. Bioremediation of PAH by *Streptomyces* sp, *Bul . Environ. Contam. Toxicol.* 86, 268-271.
- [5] Chen, S., Peng, J., Duan, G., 2016. Enrichment of functional microbes and genes during pyrene degradation in two different soils, *J Soil Sediment* 16, 417-426.

[6] Chen, S., Duan, G., Ding, K., Huang, F., Zhu, Y., 2018. DNA stable-isotope probing identifies uncultivated members of *Pseudonocardia* associated with biodegradation of pyrene in agricultural soil, *FEMS Microbiol Ecol* 94, fiy026.

[7] De, J., Ramaiah, N., Mesquita, A., Verlekar, X., 2003. Tolerance to various toxicants by marine bacteria highly resistant to mercury, *Marine Biotechnology* 5, 185-193.

[8] De, J., Ramaiah, N., 2007. Characterization of marine bacteria highly resistant to mercury exhibiting multiple resistances to toxic chemicals, *Ecological Indicators* 7, 511-520.

[9] Delgado-Baquerizo, M., Oliverio, A.M., Brewer, T.E., Benavent-Gonzalez, A., Eldridge, D.J., Bardgett, R.D., Maestre, F.T., Singh, B.K., Fierer, N., 2018. A global atlas of the dominant bacteria found in soil, *Science* 359, 320-+.

[10] Deng, S., Ke, T., Li, L., Cai, S., Zhou, Y., Liu, Y., Guo, L., Chen, L., Zhang, D., 2018. Impacts of environmental factors on the whole microbial communities in the rhizosphere of a metal-tolerant plant: *Elsholtzia haichowensis* Sun, *Environ. Pollut.* 237, 1088-1097.

[11] Denome, S.A., Stanley, D.C., Olson, E.S., Young, K.D., 1993. Metabolism of dibenzothiophene and naphthalene in *Pseudomonas* strains: complete DNA sequence of an upper naphthalene catabolic pathway, *Journal Of Bacteriology* 175, 6890-6901.

[12] Duan, L., Naidu, R., Thavamani, P., Meaklim, J., Megharaj, M., 2015. Managing long-term polycyclic aromatic hydrocarbon contaminated soils: a risk-based approach, *Environ Sci Pollut R* 22, 8927-8941.

[13] Dybas, M.J., Hyndman, D.W., Heine, R., Tiedje, J., Linning, K., Wiggert, D., Voice, T., Zhao, X., Dybas, L., Criddle, C.S., 2002. Development, operation, and long-term performance of a full-scale biocurtain utilizing bioaugmentation, *Environ Sci Technol* 36, 3635-3644.

[14] Elyamine, A.M., Kan, J., Meng, S.S., Tao, P., Wang, H., Hu, Z., 2021. Aerobic and Anaerobic Bacterial and Fungal Degradation of Pyrene: Mechanism Pathway Including Biochemical Reaction and Catabolic Genes, *Int J Mol Sci* 22.

[15] Gallego, S., Vila, J., Tauler, M., Nieto, J.M., Breugelmans, P., Springael, D., Grifoll, M., 2014. Community structure and PAH ring-hydroxylating dioxygenase genes of a marine pyrene-degrading microbial consortium, *Biodegradation* 25, 543-556.

[16] Ghosal, D., Ghosh, S., Dutta, T.K., Ahn, Y., 2016. Current state of knowledge in microbial degradation of Polycyclic Aromatic Hydrocarbons (PAHs): A review, *Front. Microbiol.* 7, 1369.

[17] Guo, C., Dang, Z., Wong, Y., Tam, N.F., 2010. Biodegradation ability and dioxygenase genes of PAH-degrading *Sphingomonas* and *Mycobacterium* strains isolated from mangrove sediments, *Int Biodeterior Biodegradation* 64, 419-426.

[18] Guo, G., Tian, F., Ding, K., Wang, L., Liu, T., Yang, F., 2017. Bacterial Communities Predominant in the Degradation of C-13-Labeled Pyrene in Red Soil, *Soil & Sediment Contamination* 26, 709-721.

[19] Haleyur, N., Shahsavari, E., Taha, M., Khudur, L.S., Koshlaf, E., Osborn, A.M., Ball, A.S., 2018. Assessing the degradation efficacy of native PAH-degrading bacteria from aged, weathered soils in an Australian former gasworks site, *Geoderma* 321, 110-117.

[20] Hall, K., Miller, C., Sorensen, D.L., Anderson, A.J., Sims, R.C., 2005. Development of a catabolically significant genetic probe for polycyclic aromatic hydrocarbon-degrading Mycobacteria in soil, *Biodegradation* 16, 475-484.

[21] Heinaru, E., Merimaa, M., Viggor, S., Lehiste, M., Leito, I., Truu, J., Heinaru, A., 2005. Biodegradation efficiency of functionally important populations selected for bioaugmentation in phenol- and oil-polluted area, *FEMS Microbiol Ecol* 51, 363-373.

[22] Im, W.T., Liu, Q.M., Yang, J.E., Kim, M.S., Kim, S.Y., Lee, S.T., Yi, T.H., 2010. *Panacagrimonas perspica* gen. nov., sp. nov., a novel member of Gammaproteobacteria isolated from soil of a ginseng field, *Journal Of Microbiology* 48, 262-266.

- [23] Izmalkova, T.Y., Sazonova, O.I., Kosheleva, I.A., Boronin, A.M., 2013. Phylogenetic Analysis of the Genes for Naphthalene and Phenanthrene Degradation in *Burkholderia* sp Strains, *Russ. J. Genet.* 49, 609-616.
- [24] Jia, X., He, Y., Huang, L., Jiang, D., Lu, W., 2019. n-Hexadecane and pyrene biodegradation and metabolization by *Rhodococcus* sp. T1 isolated from oil contaminated soil, *Chinese Journal of Chemical Engineering* 27, 411-417.
- [25] Jiang, B., Jin, N., Xing, Y., Su, Y., Zhang, D., 2018a. Unraveling uncultivable pesticide degraders via stable isotope probing (SIP), *Crit. Rev. Biotechnol.* 38, 1025-1048.
- [26] Jiang, B., Adebayo, A., Jia, J., Xing, Y., Deng, S., Guo, L., Liang, Y., Zhang, D., 2019. Impacts of heavy metals and soil properties at a Nigerian e-waste site on soil microbial community, *J Hazard Mater* 362, 187-195.
- [27] Jiang, Y., Zhang, Z., Zhang, X., 2018b. Co-biodegradation of pyrene and other PAHs by the bacterium *Acinetobacter johnsonii*, *Ecotox Environ Safe* 163, 465-470.
- [28] Jin, J., Yao, J., Zhang, Q., 2016a. Biodegradation of Phenanthrene by *Pseudomonas* sp JPN2 and Structure-Based Degrading Mechanism Study, *Bulletin of Environmental Contamination and Toxicology* 97, 689-694.

[29] Jin, J., Yao, J., Zhang, Q., Liu, J., 2016b. Biodegradation of pyrene by pseudomonas sp JPN2 and its initial degrading mechanism study by combining the catabolic nahAc gene and structure-based analyses, *Chemosphere* 164, 379-386.

[30] Johnsen, A.R., Wick, L.Y., Harms, H., 2005. Principles of microbial PAH-degradation in soil, *Environ Pollut* 133, 71-84.

[31] Jurelevicius, D., Alvarez, V.M., Peixoto, R., Rosado, A.S., Seldin, L., 2012. Bacterial polycyclic aromatic hydrocarbon ring-hydroxylating dioxygenases (PAH-RHD) encoding genes in different soils from King George Bay, Antarctic Peninsula, *Appl Soil Ecol* 55, 1-9.

[32] Kaeberlein, T., Lewis, K., Epstein, S.S., 2002. Isolating "uncultivable" microorganisms in pure culture in a simulated natural environment, *Science* 296, 1127-1129.

[33] Kalyuzhnaya, M.G., Beck, D.A.C., Suci, D., Pozhitkov, A., Lidstrom, M.E., Chistoserdova, L., 2010. Functioning in situ: gene expression in *Methylobacterium mobilis* in its native environment as assessed through transcriptomics, *ISME J* 4, 388-398.

[34] Kanaly, R.A., Harayama, S., 2000. Biodegradation of high-molecular-weight polycyclic aromatic hydrocarbons by bacteria, *Journal Of Bacteriology* 182, 2059-2067.

[35] Kashyap, N., Moholkar, V.S., 2021. Intensification of pyrene degradation by native *Candida tropicalis* MTCC 184 with sonication: Kinetic and mechanistic investigation, *Chemical Engineering and Processing-Process Intensification* 164.

[36] Khan, A.A., Wang, R., Cao, W., Doerge, D.R., Wennerstrom, D., Cerniglia, C.E., 2001. Molecular cloning, nucleotide sequence, and expression of genes encoding a polycyclic aromatic ring dioxygenase from *Mycobacterium* sp strain PYR-1, *Appl. Environ. Microbiol.* 67, 3577-3585.

[37] Khan, S., Gupta, S., Gupta, N., 2018. Dearomatization of diesel oil using *Pseudomonas* sp, *Biotechnology letters* 40, 1329-1333.

[38] Kim, K.-H., Jahan, S.A., Kabir, E., Brown, R.J.C., 2013. A review of airborne polycyclic aromatic hydrocarbons (PAHs) and their human health effects, *Environ Int* 60, 71-80.

[39] Krivobok, S., Kuony, S., Meyer, C., Louwagie, M., Willison, J.C., Jouanneau, Y., 2003. Identification of pyrene-induced proteins in *Mycobacterium* sp strain 6PY1: Evidence for two ring-hydroxylating dioxygenases, *Journal Of Bacteriology* 185, 3828-3841.

[40] Li, C., Hu, H., Chen, Q., Chen, D., He, J., 2019. *Comammox Nitrospira* play an active role in nitrification of agricultural soils amended with nitrogen fertilizers, *Soil Biol Biochem* 138, 107609.

[41] Li, J., Luo, C., Zhang, D., Song, M., Cai, X., Jiang, L., Zhang, G., 2018a. Autochthonous Bioaugmentation-Modified Bacterial Diversity of Phenanthrene Degraders in PAH-Contaminated Wastewater as Revealed by DNA-Stable Isotope Probing, *Environ Sci Technol* 52, 2934-2944.

[42] Li, J., Luo, C., Zhang, G., Zhang, D., 2018b. Coupling magnetic-nanoparticle mediated isolation (MMI) and stable isotope probing (SIP) for identifying and isolating the active microbes involved in phenanthrene degradation in wastewater with higher resolution and accuracy, *Water Res* 144, 226-234.

[43] Liang, Y., Gardner, D.R., Miller, C.D., Chen, D., Anderson, A.J., Weimer, B.C., Sims, R.C., 2006. Study of biochemical pathways and enzymes involved in pyrene degradation by *Mycobacterium* sp strain KMS, *Appl. Environ. Microbiol.* 72, 7821-7828.

[44] Liu, T., Xu, Y., Liu, H., Luo, S., Yin, Y., Liu, S., Zhou, N., 2011. Functional characterization of a gene cluster involved in gentisate catabolism in *Rhodococcus* sp. strain NCIMB 12038, *Applied Microbiology and Biotechnology* 90, 671-678.

[45] Liu, Y., Gao, P., Su, J., da Silva, E.B., de Oliveira, L.M., Townsend, T., Xiang, P., Ma, L.Q., 2019. PAHs in urban soils of two Florida cities: Background concentrations, distribution, and sources, *Chemosphere* 214, 220-227.

[46] Lu, J., Guo, C., Li, J., Zhang, H., Lu, G., Dang, Z., Wu, R., 2013. A fusant of *Sphingomonas* sp. GY2B and *Pseudomonas* sp. GP3A with high capacity of

degrading phenanthrene, *World Journal of Microbiology and Biotechnology* 29, 1685-1694.

[47] Luan, T., Yu, K.S.H., Zhong, Y., Zhou, H., Lan, C., Tam, N.F.Y., 2006. Study of metabolites from the degradation of polycyclic aromatic hydrocarbons (PAHs) by bacterial consortium enriched from mangrove sediments, *Chemosphere* 65, 2289-2296.

[48] Macleod, C.J.A., Semple, K.T., 2006. The influence of single and multiple applications of pyrene on the evolution of pyrene catabolism in soil, *Environ Pollut* 139, 455-460.

[49] Major, D.W., McMaster, M.L., Cox, E.E., Edwards, E.A., Dworatzek, S.M., Hendrickson, E.R., Starr, M.G., Payne, J.A., Buonamici, L.W., 2002. Field demonstration of successful bioaugmentation to achieve dechlorination of tetrachloroethene to ethene, *Environ Sci Technol* 36, 5106-5116.

[50] Martiny, A.C., 2019. High proportions of bacteria are culturable across major biomes, *The ISME Journal* 13, 2125-2128.

[51] Mohanrasu, K., Premnath, N., Prakash, G.S., Sudhakar, M., Boobalan, T., Arun, A., 2018. Exploring multi potential uses of marine bacteria; an integrated approach for PHB production, PAHs and polyethylene biodegradation, *J. Photochem. Photobiol. B-Biol.* 185, 55-65.

[52] Mrozik, A., Piotrowska-Seget, Z., 2010. Bioaugmentation as a strategy for cleaning up of soils contaminated with aromatic compounds, *Microbiological research* 165, 363-375.

[53] Mustakhimov, I., Kalyuzhnaya, M.G., Lidstrom, M.E., Chistoserdova, L., 2013. Insights into Denitrification in *Methylothermobacter mobilis* from Denitrification Pathway and Methanol Metabolism Mutants, *Journal Of Bacteriology* 195, 2207-2211.

[54] Nam, J.J., Thomas, G.O., Jaward, F.M., Steinnes, E., Gustafsson, O., Jones, K.C., 2008. PAHs in background soils from Western Europe: Influence of atmospheric deposition and soil organic matter, *Chemosphere* 70, 1596-1602.

[55] Navarro-Noya, Y.E., Jan-Roblero, J., del Carmen González-Chávez, M., Hernández-Gama, R., Hernández-Rodríguez, C., 2010. Bacterial communities associated with the rhizosphere of pioneer plants (*Bahia xyloperda* and *Viguiera linearis*) growing on heavy metals-contaminated soils, *Antonie Van Leeuwenhoek* 97, 335-349.

[56] Nzila, A., 2013. Update on the cometabolism of organic pollutants by bacteria, *Environ Pollut* 178, 474-482.

[57] Nzila, A., Sankara, S., Al-Momani, M., Musa, M.M., 2018. Isolation and characterisation of bacteria degrading polycyclic aromatic hydrocarbons: phenanthrene and anthracene, *Archives of Environmental Protection* 44, 43-54.

[58] Obayori, O.S., Salam, L.B., Oyetibo, G.O., Idowu, M., Amund, O.O., 2017. Biodegradation potentials of polyaromatic hydrocarbon (pyrene and phenanthrene) by *Proteus mirabilis* isolated from an animal charcoal polluted site, *Biocatalysis and Agricultural Biotechnology* 12, 78-84.

[59] Okere, U.V., Schuster, J.K., Ogbonnaya, U.O., Jones, K.C., Semple, K.T., 2017. Indigenous C-14-phenanthrene biodegradation in "pristine" woodland and grassland soils from Norway and the United Kingdom, *Environ Sci-Proc Imp* 19, 1437-1444.

[60] Peng, R., Xiong, A., Xue, Y., Fu, X., Gao, F., Zhao, W., Tian, Y., Yao, Q., 2008. Microbial biodegradation of polyaromatic hydrocarbons, *FEMS Microbiology Review* 32, 927-955.

[61] Perelo, L.W., 2010. Review: In situ and bioremediation of organic pollutants in aquatic sediments, *J Hazard Mater* 177, 81-89.

[62] Pinyakong, O., Habe, H., Yoshida, T., Nojiri, H., Omori, T., 2003. Identification of three novel salicylate 1-hydroxylases involved in the phenanthrene degradation of *Sphingobium* sp strain P2, *Biochemical and biophysical research communications* 301, 350-357.

[63] Rabodonirina, S., Rasolomampianina, R., Krier, F., Drider, D., Merhaby, D., Net, S., Ouddane, B., 2018. Degradation of fluorene and phenanthrene in

PAHs-contaminated soil using *Pseudomonas* and *Bacillus* strains isolated from oil spill sites, *J Environ Manage* 232, 1-7.

[64] Ren, X., Zeng, G., Tang, L., Wang, J., Wan, J., Liu, Y., Yu, J., Yi, H., Ye, S., Deng, R., 2018. Sorption, transport and biodegradation - An insight into bioavailability of persistent organic pollutants in soil, *Sci Total Environ* 610, 1154-1163.

[65] Sørensen, S.J., Tim, S., Regin, R., 1999. Predation by protozoa on *Escherichia coli* K12 in soil and transfer of resistance plasmid RP4 to indigenous bacteria in soil, *Appl Soil Ecol* 11, 79-90.

[66] Saito, A., Iwabuchi, T., Harayama, S., 1999. Characterization of genes for enzymes involved in the phenanthrene degradation in *Nocardioides* sp. KP7, *Chemosphere* 38, 1331-1337.

[67] Sakshi, Singh, S.K., Haritash, A.K., 2021. Catabolic enzyme activity and kinetics of pyrene degradation by novel bacterial strains isolated from contaminated soil, *Environmental Technology & Innovation* 23.

[68] Schimel, J.P., Schaeffer, S.M., 2012. Microbial control over carbon cycling in soil, *Frontiers in Microbiology* 3, 348.

[69] Schuler, L., Chadhain, S.M.N., Jouanneau, Y., Meyer, C., Zylstra, G.J., Hols, P., Agathos, S.N., 2008. Characterization of a novel angular dioxygenase from

fluorene-degrading *Spingomonas* sp strain LB126, *Appl. Environ. Microbiol.* 74, 1050-1057.

[70] Segura, A., Hernandez-Sanchez, V., Marques, S., Molina, L., 2017. Insights in the regulation of the degradation of PAHs in *Novosphingobium* sp HR1a and utilization of this regulatory system as a tool for the detection of PAHs, *Sci Total Environ* 590, 381-393.

[71] Song, M., Luo, C., Jiang, L., Zhang, D., Wang, Y., Zhang, G., Nojiri, H., 2015. Identification of Benzo[a]pyrene-Metabolizing Bacteria in Forest Soils by Using DNA-Based Stable-Isotope Probing, *Appl. Environ. Microbiol.* 81, 7368-7376.

[72] Stingley, R.L., Khan, A.A., Cerniglia, C.E., 2004. Molecular characterization of a phenanthrene degradation pathway in *Mycobacterium vanbaalenii* PYR-1, *Biochemical and biophysical research communications* 322, 133-146.

[73] Sun, S., Wang, H., Chen, Y., Lou, J., Wu, L., Xu, J., 2019. Salicylate and phthalate pathways contributed differently on phenanthrene and pyrene degradations in *Mycobacterium* sp. WY10, *J Hazard Mater* 364, 509-518.

[74] Sun, Y., Yin, M., Zheng, D., Wang, T., Zhao, X., Luo, C., Li, J., Liu, Y., Xu, S., Deng, S., Wang, X., Zhang, D., 2021. Different acetonitrile degraders and degrading genes between anaerobic ammoniumoxidation and sequencing batch

reactor as revealed by stable isotope probing and magnetic-nanoparticle mediated isolation, *Sci. Total Environ.* 758, 143588.

[75] Takizawa, N., Iida, T., Sawada, T., Yamauchi, K., Wang, Y.W., Fukuda, M., Kiyohara, H., 1999. Nucleotide sequences and characterization of genes encoding naphthalene upper pathway of *Pseudomonas aeruginosa* PaK1 and *Pseudomonas putida* OUS82, *Journal of Bioscience and Bioengineering* 87, 721-731.

[76] Tang, Y., Long, X., Wu, M., Yang, S., Gao, N., Xu, B., Dutta, S., 2020. Bibliometric Review of Research Trends on Disinfection By-Products in Drinking Water during 1975-2018, *Sep Purif Technol* 116741.

[77] Tao, X., Lu, G., Dang, Z., Yang, C., Yi, X., 2007. A phenanthrene-degrading strain *Sphingomonas* sp GY2B isolated from contaminated soils, *Process Biochemistry* 42, 401-408.

[78] Thompson, I.P., van der Gast, C.J., Ciric, L., Singer, A.C., 2005. Bioaugmentation for bioremediation: the challenge of strain selection, *Environmental Microbiology* 7, 909-915.

[79] Ukalska-Jaruga, A., Debaene, G., Smreczak, B.O.D., 2020. Dissipation and sorption processes of polycyclic aromatic hydrocarbons (PAHs) to organic matter in soils amended by exogenous rich-carbon material, *J Soil Sediment* 20, 836-849.

[80] Vaidya, S., Jain, K., Madamwar, D., 2017. Metabolism of pyrene through phthalic acid pathway by enriched bacterial consortium composed of *Pseudomonas*, *Burkholderia*, and *Rhodococcus* (PBR), 3 Biotech 7, 29.

[81] van Herwijnen, R., Wattiau, P., Bastiaens, L., Daal, L., Jonker, L., Springael, D., Govers, H.A.J., Parsons, J.R., 2003. Elucidation of the metabolic pathway of fluorene and cometabolic pathways of phenanthrene, fluoranthene, anthracene and dibenzothiophene by *Sphingomonas* sp LB126, Research in Microbiology 154, 199-206.

[82] Vartoukian, S.R., Palmer, R.M., Wade, W.G., 2010. Strategies for culture of 'unculturable' bacteria, FEMS Microbiology Letters 309, 1-7.

[83] Wang, B., Teng, Y., Xu, Y., Chen, W., Ren, W., Li, Y., Christie, P., Luo, Y., 2018. Effect of mixed soil microbiomes on pyrene removal and the response of the soil microorganisms, Sci Total Environ 640, 9-17.

[84] Wang, C., Wu, S., Zhou, S., Sill, Y., Song, J., 2017a. Characteristics and Source Identification of Polycyclic Aromatic Hydrocarbons (PAHs) in Urban Soils: A Review, Pedosphere 27, 17-26.

[85] Wang, J., Zhang, X., Ling, W., Liu, R., Liu, J., Kang, F., Gao, Y., 2017b. Contamination and health risk assessment of PAHs in soils and crops in industrial areas of the Yangtze River Delta region, China, Chemosphere 168, 976-987.

[86] Wang, X., Zhao, X., Li, H., Jia, J., Liu, Y., Ejenavi, O., Ding, A., Sun, Y., Zhang, D., 2016a. Separating and characterizing functional alkane degraders from crude-oil-contaminated sites via magnetic nanoparticle-mediated isolation, *Res. Microbiol.* 167, 731-744.

[87] Wang, Y., Huang, W.E., Cui, L., Wagner, M., 2016b. Single cell stable isotope probing in microbiology using Raman microspectroscopy, *Current Opinion in Biotechnology* 41, 34-42.

[88] Wang, Z., Cao, Y., Zhu-Barker, X., Nicol, G.W., Wright, A.L., Jia, Z., Jiang, X., 2019. *Comammox Nitrospira* clade B contributes to nitrification in soil, *Soil Biol Biochem* 135, 392-395.

[89] Wu, F., Guo, C., Liu, S., Liang, X., Lu, G., Dang, Z., 2019. Pyrene Degradation by *Mycobacterium gilvum*: Metabolites and Proteins Involved, *Water Air Soil Poll* 230, 67.

[90] Wu, H., Shen, J., Jiang, X., Liu, X., Sun, X., Li, J., Han, W., Wang, L., 2018. Bioaugmentation strategy for the treatment of fungicide wastewater by two triazole-degrading strains, *Chem Eng J* 349, 17-24.

[91] Zafra, G., Absalón, Á.E., Anducho-Reyes, M.Á., Fernandez, F.J., Cortés-Espinosa, D.V., 2017. Construction of PAH-degrading mixed microbial consortia by induced selection in soil, *Chemosphere* 172, 120-126.

[92] Zeng, J., Zhu, Q., Wu, Y., Chen, H., Lin, X., 2017. Characterization of a polycyclic aromatic ring-hydroxylation dioxygenase from *Mycobacterium* sp NJS-P, *Chemosphere* 185, 67-74.

[93] Zhang, D., Fakhrullin, R.F., Özmen, M., Wang, H., Wang, J., Paunov, V.N., Li, G., Huang, W.E., 2011. Functionalization of whole-cell bacterial reporters with magnetic nanoparticles, *Microb Biotechnol* 4, 89-97.

[94] Zhang, D., He, Y., Wang, Y., Wang, H., Wu, L., Aries, E., Huang, W.E., 2012. Whole-cell bacterial bioreporter for actively searching and sensing of alkanes and oil spills, *Microb Biotechnol* 5, 87-97.

[95] Zhang, D., Berry, J.P., Zhu, D., Wang, Y., Chen, Y., Jiang, B., Huang, S., Langford, H., Li, G., Davison, P.A., Xu, J., Aries, E., Huang, W.E., 2015. Magnetic nanoparticle-mediated isolation of functional bacteria in a complex microbial community, *Isme Journal* 9, 603-614.

[96] Zhao, H., Zhang, Y., Xiao, X., Li, G., Zhao, Y., Liang, Y., 2017. Different phenanthrene-degrading bacteria cultured by in situ soil substrate membrane system and traditional cultivation, *Int Biodeterior Biodegradation* 117, 269-277.

[97] Zhao, X., Li, H., Ding, A., Zhou, G., Sun, Y., Zhang, D., 2016. Preparing and characterizing Fe<sub>3</sub>O<sub>4</sub>@cellulose nanocomposites for effective isolation of cellulose-decomposing microorganisms, *Mater Lett* 163, 154-157.

[98] Zhong, J., Luo, L., Chen, B., Sha, S., Qing, Q., Tam, N., Zhang, Y., Luan, T., 2017. Degradation pathways of 1-methylphenanthrene in bacterial *Sphingobium* sp MP9-4 isolated from petroleum-contaminated soil, *Marine Pollution Bulletin* 114, 926-933.

[99] Zhong, Y., Luan, T., Zhou, H., Lan, C., Tam, N., 2006. Metabolite production in degradation of pyrene alone or in a mixture with another polycyclic aromatic hydrocarbon by *Mycobacterium* sp, *Environ Toxicol Chem* 25, 2853-2859.

[100] Zhou, H., Guo, C., Wong, Y.S., Tam, N., 2006. Genetic diversity of dioxygenase genes in polycyclic aromatic hydrocarbon-degrading bacteria isolated from mangrove sediments, *FEMS Microbiology Letters* 262, 148-157.

[101] Zhou, H., Wang, H., Huang, Y., Fang, T., 2016. Characterization of pyrene degradation by halophilic *Thalassospira* sp strain TSL5-1 isolated from the coastal soil of Yellow Sea, China, *Int Biodeterior Biodegradation* 107, 62-69.

## Figure captions

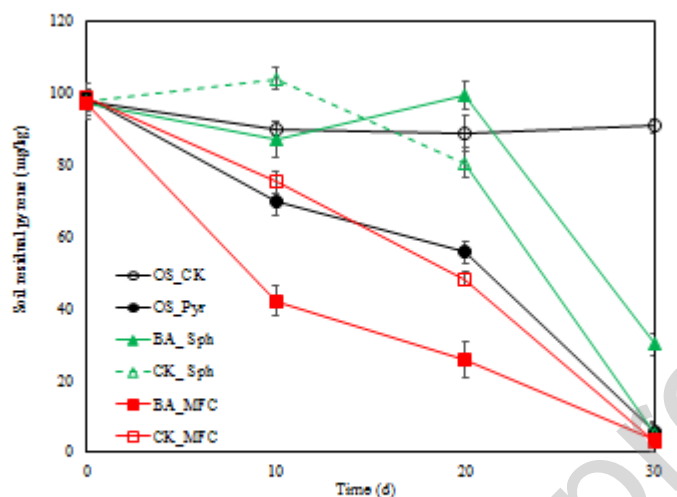


**Figure 1**

**Figure 1.** Pyrene degradation curves in different treatments. OS\_CK represents the sterile soils with pyrene amendment. OS\_Pyr represents the original soil treatments with pyrene amendment. BA\_Sph refers to bioaugmentation treatment with original soils, pyrene and *Sphingomonas* sp. YT1005. CK\_Sph refers to bioaugmentation treatment with sterile soils, pyrene and *Sphingomonas* sp. YT1005. BA\_MFC refers to bioaugmentation treatment with original soils, pyrene and MMI-enriched pyrene degrading consortium. CK\_MFC refers to bioaugmentation treatment with sterile soils, pyrene and MMI-enriched pyrene degrading consortium.

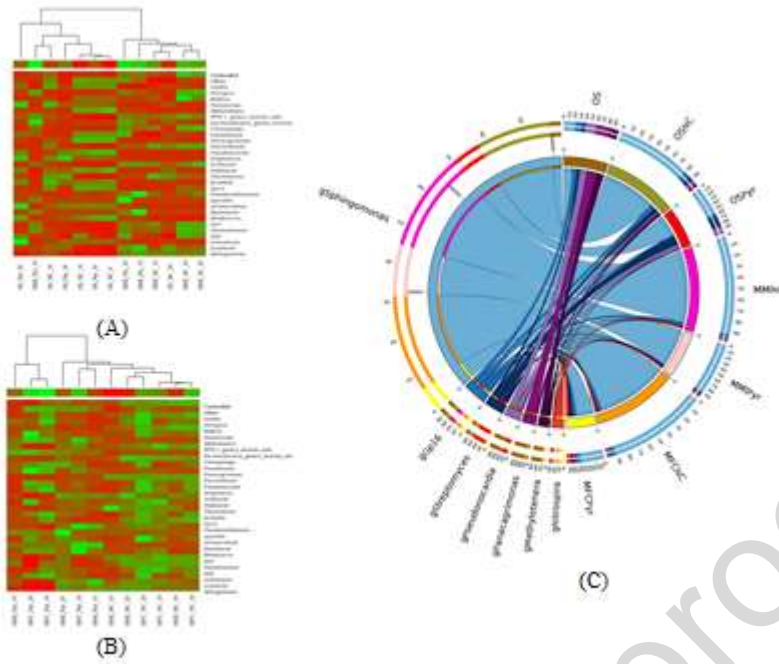


**Figure 2**

**Figure 2.** (A) Bray-Curtis metric distance of bacterial community compositions between OS\_NC, OS\_Pyr, MMI\_NC and MMI\_Pyr treatments on genus level. (B) Bray-Curtis metric distance of bacterial community compositions between MMI\_NC, MMI\_Pyr, MFC\_NC and MFC\_Pyr treatments on genus level. Color blocks represent the relative abundance of each bacterial general, wherein the redder color indicates the higher relative abundance. ‘\_10’, ‘\_20’ and ‘\_30’ represented samples collected on 10, 20 and 30 days, respectively.

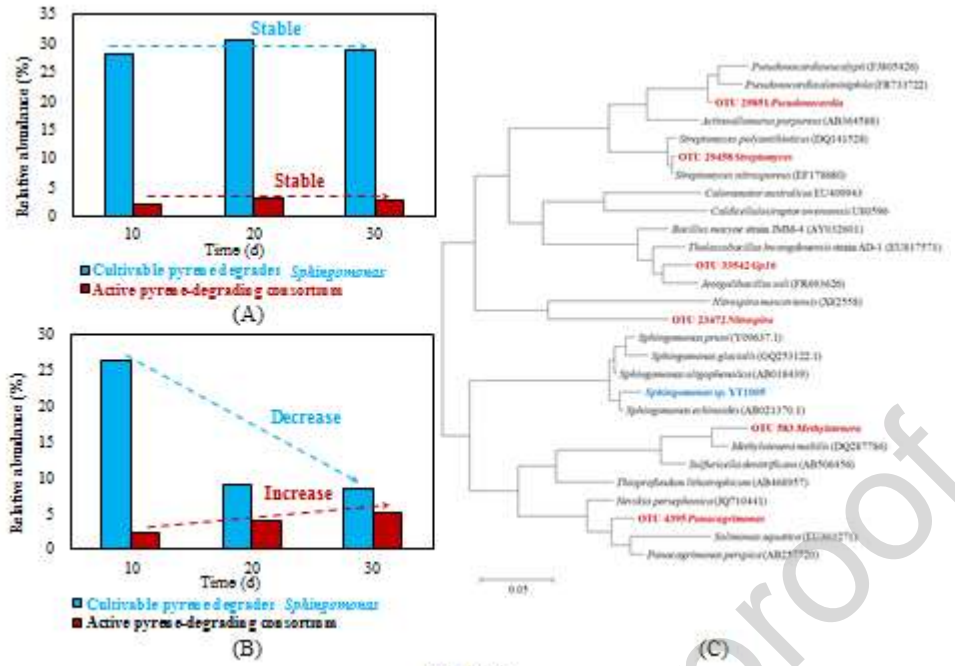
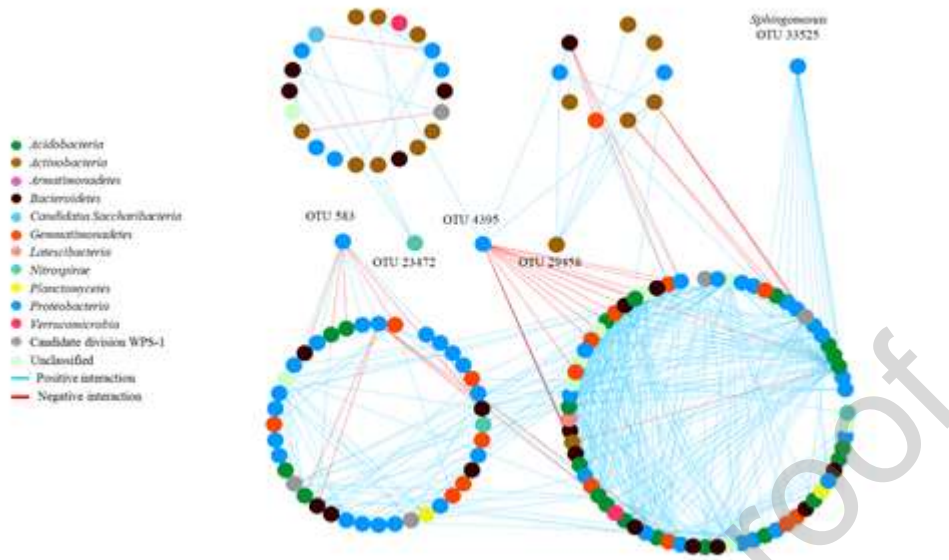


Figure 3

**Figure 3.** (A) The relative abundance of *Spingomonas* sp. YT1005 and the active pyrene degraders in MFC\_NC (no pyrene) throughout the incubation process. (B) The relative abundance of *Spingomonas* sp. YT1005 and the active pyrene degraders in MFC\_Pyr (amendment with pyrene) throughout the incubation process. (C) The phylogenetic tree of cultivable pyrene degrader *Spingomonas* sp. YT1005 (OTU33525) and the potential active pyrene degraders, including *Nitrospira* (OTU23472), *Gp16* (OTU33542), *Streptomyces* (OTU29458), *Pseudonocardia* (OTU29851), *Panacagrimonas* (OTU4395) and *Methylotenera* (OTU583).



**Figure 4**

**Figure 4.** The co-occurrence molecular ecological network constructed based on core OTUs with the abundance  $> 0.5\%$  and occurrence in over 10 of all 19 samples. Blue and red edges represent positive or negative correlations, respectively. Each point (node) stands for one OTU and the edges represent the correlations between connected OTUs. Only the modules with member number  $> 5$  and correlated with cultivable or active pyrene-degraders were kept. OTU33525 represents the cultivable pyrene degrader *Sphingomonas* sp. YT1005. Core OTUs representing the active pyrene degraders include *Nitrospira* (OTU23472), *Streptomyces* (OTU29458), *Panacagrimonas* (OTU4395) and *Methylotenera* (OTU583). The other two active pyrene degraders, *Gp16* (OTU33542) and *Pseudonocardia* (OTU29851), are not core OTUs in the molecular ecological network and not illustrated.

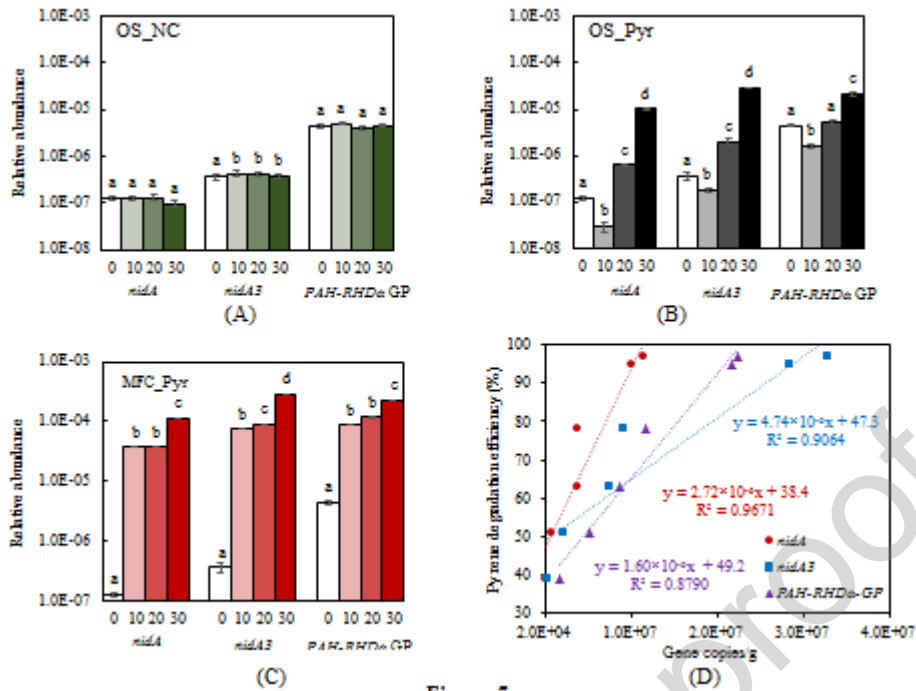
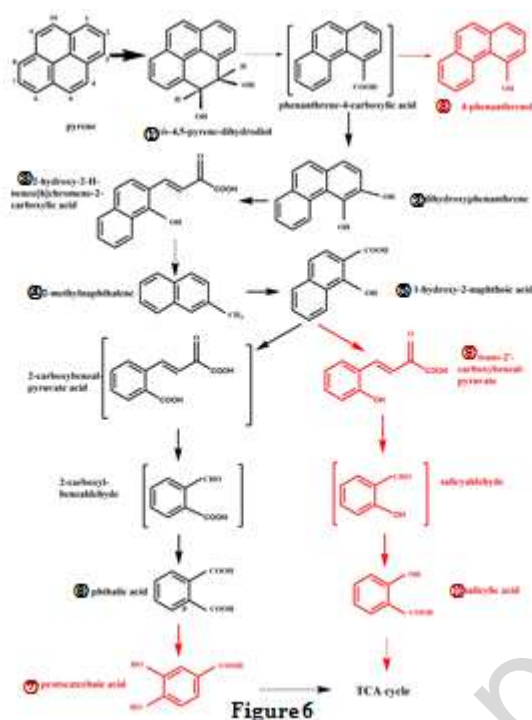


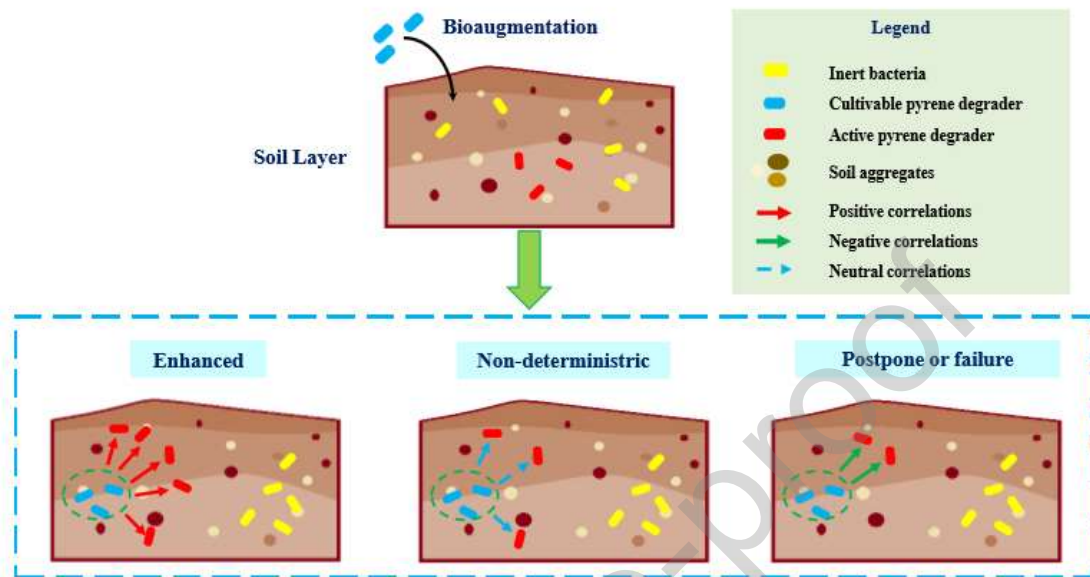
Figure 5

**Figure 5.** The relative abundance of pyrene dioxygenase encoding genes (*nidA*, *nidA3* and PAH-RHD $\alpha$ -GP) in OS\_NC (A), OS\_Pyr (B) and MFC\_Pyr (C) treatments during 30-day pyrene degradation process. (D) Correlations between pyrene degradation efficiency and the relative abundance of pyrene dioxygenase encoding genes (*nidA*, *nidA3* and PAH-RHD $\alpha$ -GP). Short dash line represents the logarithmic nonlinear regression of *nidA* gene; long dash line represents the logarithmic nonlinear regression of *nidA3* gene; dotted line represents the logarithmic nonlinear regression of PAH-RHD $\alpha$ -GP gene.



**Figure 6.** Pyrene degradation metabolites and pathways by the cultivable degraders *Sphingomonas* sp. YT1005 and MMI-enriched active pyrene degrading consortium. Dash arrows represent multiple metabolic steps. Bracketed compounds are hypothetical metabolites not identified in the present study. Compounds in black color are metabolites identified in both NC\_Sph and NC\_MFC treatments, following the phthalate pathway. Compounds in red color are metabolites identified only in NC\_MFC treatments, following the salicylate pathway.

## Graphical abstract



### **CRedit author statement**

**Bo Jiang:** Methodology, Resources, Data curation, Writing-Original draft preparation.

**Yating Chen:** Investigation, Writing-Original draft preparation.

**Yi Xing:** Validation, Writing-Original draft preparation.

**Luning Lian:** Investigation, Validation.

**Yaixin Shen:** Investigation, Validation.

**Baogang Zhang:** Methodology, Resources.

**Han Zhang:** Methodology, Resources.

**Guangdong Sun:** Methodology, Resources.

**Junyi Li:** Methodology, Resources.

**Xinzi Wang:** Methodology, Resources.

**Dayi Zhang:** Conceptualization, Formal analysis, Data curation, Writing-Original draft preparation, Writing-Reviewing and Editing.

---

**Declaration of interests**

The authors declare that they have no known competing financial interests or personal relationships that could have appeared to influence the work reported in this paper.

The authors declare the following financial interests/personal relationships which may be considered as potential competing interests:

---

## Highlights

- Postponed pyrene degradation by cultivable *Sphingomonas* sp. YT1005
- Accelerated pyrene degradation by MMI-enriched active pyrene degraders
- Postponed pyrene degradation was explained by negative intraspecies correlations
- Phthalate pathway in YT1005 and phthalate/salicylate pathways by active degraders
- MMI is suitable to enrich the active-yet-uncultivable degraders for bioaugmentation